Neuropsychologia 155 (2021) 107821

Contents lists available at ScienceDirect

Neuropsychologia

journal homepage: http://www.elsevier.com/locate/neuropsychologia

Brain-behavior relationships in the perceptual decision-making process through cognitive processing stages

Elaheh Imani [a], Ahad Harati [a], Hamidreza Pourreza [a,*], Morteza Moazami Goudarzi [b,**]

[a] Department of Computer Engineering, Ferdowsi University of Mashhad, Mashhad, Iran
[b] The Picower Institute for Learning and Memory, Department of Brain and Cognitive Sciences, Massachusetts Institute of Technology, Cambridge, MA, 02139, USA

ARTICLE INFO

Keywords:
Perceptual decision making
Neural and behavioral characterizations
Cognitive processing stages

ABSTRACT

Perceptual decision making – the process of detecting and categorizing information – has been studied extensively over the last two decades. In this study, we aim to bridge the gap between neural and behavioral representations of the perceptual decision-making process. The neural characterization of decision-making was investigated by evaluating the duration and neural signature of the information processing stages. We further evaluated the processing stages of the decision-making process at the behavioral level by estimating the drift rate and non-decision time parameters. We asked whether the neural and behavioral characterizations of the decision-making process provided consistent results under different stimulus coherency levels and spatial attention. Our statistical analysis revealed that, at both representational levels, decision-making was affected more by the coherency factor. We further found that among different information processing stages, the decision stage had the highest role in the performance of the decision-making process. Such that, the shorter decision stage duration at the neural level and higher drift rate at the behavioral level lead to faster decision-making. Through our consistent neural and behavioral results, we have shown that the decision-making components at these two representational levels were significantly associated. Moreover, the neural signature of the processing stages gave information about the regions that contributed more to the decision-making process. Our overall results demonstrate that uncovering the cognitive processing stages provided more insights into the decision-making process.

1. Introduction

In daily work, people often encounter scenarios in which they must select an action based on noisy sensory inputs. The process of choosing an action based on noisy sensory information is called perceptual decision-making. Different processing stages are needed to receive sensory information, accumulate perceptual evidence, and map sensory inputs to motor actions to accomplish the decision-making process in the brain (Sterzer, 2016; Siegel et al., 2011). Various computational models have been proposed to describe the decision-making process at the behavioral level based on reaction time (RT) and response accuracy (Ratcliff and Smith, 2004; Smith and Ratcliff, 2004; Usher and McClelland, 2001; Brown and Heathcote, 2008/11). Accumulating the noisy perceptual evidence overtime to reach the decision boundary before the response execution is the common idea across these models. Since this process is inherently noisy, the decision-making system needs time to collect enough evidence to make a decision (Ratcliff and McKoon, 2008). Several researchers have investigated the neural underpinnings of this evidence accumulation process. Initial analysis using single cell recordings in non-human primates (NHP) trained to perform visual decision-making tasks have suggested that individual neurons are implicated in this evidence accumulation process (Roitman and Shadlen, 2002; Gold and Shadlen, 2001; Gold and Shadlen, 2000/03). Notably, experiments on monkeys have revealed that neurons in the lateral intraparietal (LIP) cortex (Roitman and Shadlen, 2002), frontal eye field (FEF) (Mante et al., 2013/11), striatum (Ding and Gold, 2010), and superior colliculus (Horwitz and Newsome, 1999) had a ramped up firing rate profile to reach the decision boundary. These neurons integrate the information received from sensory areas over time to reach the decision boundary. Moreover, the analysis of the single set recording in rodents uncovered that neurons in the posterior parietal cortex (PPC) and frontal orienting field (FOF) had a role in the evidence accumulation

* Corresponding author.
** Corresponding author.
E-mail addresses: hpourreza@um.ac.ir (H. Pourreza), moazami@mit.edu (M.M. Goudarzi).

https://doi.org/10.1016/j.neuropsychologia.2021.107821
Received 17 May 2020; Received in revised form 4 January 2021; Accepted 2 March 2021
Available online 5 March 2021
0028-3932/

process (Hanks et al., 2015; Scott et al., 2017).

Later approaches described the decision-making process at both the behavioral and physiological levels on human subjects with more complex tasks. Non-invasive imaging of human subjects, such as functional magnetic resonance imaging (fMRI) and magneto/electroencephalography (M/EEG), gave researchers the ability to characterize the decision-making process at a whole-brain level (Hanks and Summerfield, 2017/01; Mulder et al., 2014). The studies in this area investigated the association between decision-making parameters with fMRI and EEG data. The fMRI data with its high spatial resolution was employed to discover the brain regions that were functionally involved in the decision-making process (Heekeren et al., 2004/10; Philiastides and Sajda, 2007; Binder et al., 2004/03; Liu and Pleskac, 2011; Grinband et al., 2006/03; Ho et al., 2009; Whiteet al., 2014; Pedersen et al., 2015; Pisauro et al., 2017; Veen et al., 2008; van Maanenet al., 2011; Forstmannet al., 2008; Winkelet al., 2012-). In contrast, EEG data with higher temporal resolution characterized this process with millisecond precision (Pisauro et al., 2017; O'Connell et al., 1729; van Vugt et al., 1715; Kelly and O'Connell, 2013; Tagliabue et al., 2019; van Vugt et al., 2012; Donner et al., 1581; Cavanaghet al., 1462; Herz et al., 2016). The research on the fMRI data reported the involvement of regions, such as the left dorsolateral prefrontal cortex (Heekeren et al., 2004/10), lateral occipital cortex (Philiastides and Sajda, 2007), anterior Insula (Binder et al., 2004/03; Liu and Pleskac, 2011; Grinband et al., 2006/03), inferior frontal sulcus (Liu and Pleskac, 2011), right Insula (Ho et al., 2009), right inferior frontal gyrus (Whiteet al., 2014; Pedersen et al., 2015), medial frontal gyrus (Whiteet al., 2014), posterior-medial frontal cortex (Pisauro et al., 2017), and dorsomedial prefrontal cortex (Pedersen et al., 2015), responsible for evidence accumulation. Other studies reported the neural correlate of the decision boundary by changing the speed-accuracy tradeoff. They found that regions including the premotor area (Veen et al., 2008; Forstmannet al., 2008; Winkelet al., 2012-), striatum (Forstmannet al., 2008; Winkelet al., 2012-), basal ganglia, thalamus, dorsolateral prefrontal (Veen et al., 2008), and dorsal anterior cingulate (van Maanenet al., 2011) had higher activations when preparing for fast rather than accurate decisions.

On the other hand, studies on the EEG data discovered the centro-parietal positivity (CPP) (O'Connell et al., 1729; van Vugt et al., 1715; Kelly and O'Connell, 2013; Tagliabue et al., 2019) and posterior parietal positivity (Pisauro et al., 2017) gradually growing until response execution as the sensory accumulation process. Also, parietal theta (van Vugt et al., 2012) and the motor cortex' beta oscillation powers (Donner et al., 1581) were related to the evidence accumulation. The studies of the neural basis of the decision boundary revealed an association between the power activity of the medial prefrontal cortex at theta frequency band and the value of decision boundary (Cavanaghet al., 1462; Herz et al., 2016).

Previous analysis of rodents' physiological and calcium imaging data revealed that perceptual decision-making was a distributed process (Steinmetz et al., 2019/12; Zatka-Haas et al., 2018). These studies showed that several brain areas contributed to the decision-making process, which was activated sequentially from visual to frontal regions. While the decision-making process consists of multiple processing stages, the previous research on the neural correlates of decision-making only described part of this process. Recently some mathematical models were introduced to decompose cognitive processes to small processing stages. These methods employed an unsupervised approach such as the hidden Markov model (HMM) to separate different processing stages by using brain activity (Borst and Anderson, 2015; Anderson et al., 2016), brain network (Vidaurreet al., 2018/07; Vidaurre et al., 2016; Stevneret al., 2019/03), or stimulus decoding models (Vidaurre et al., 2019). Such approaches provided the possibility to describe the recovered stages in terms of specific signatures. Borst and Anderson (Borst and Anderson, 2015; Anderson et al., 2016) utilized the HMM and EEG amplitude to uncover the memory retrieval processing stages. HMM's recovered states were assessed based on signature and duration to assign to each cognitive stage of the process. Vidaurre et al. (2019) employed a variable functional decoding model that characterized the relation between stimulus and EEG activity. They argued that there was no consistent timing of the processing stages across trials and utilized the HMM to extract each decoding model's timing. Other studies decomposed the resting brain state to the short-lived states with a distinct oscillatory pattern using MEG data and HMM (Vidaurreet al., 2018/07). Such frameworks provide a mechanism to characterize the processing stages of the cognitive processes at the physiological layer. However, for a more complete explanation of the cognitive process, it would be better to combine both physiological and behavioral information.

In this study, we employed a new approach to bridge this gap by discovering the association between physiological data and behavioral components, such as evidence accumulation. Accordingly, the decision-making process was decomposed into different cognitive processing stages similar to (Borst and Anderson, 2015) at the physiological level. The behavioral components of the decision-making were similarly estimated using the drift-diffusion model (DDM). We then clarified the association between neural and behavioral characterizations of the decision-making process. Using this approach, we assessed the effect of the internal subject state (spatial prioritization) and external world state (stimulus coherency) on the whole process of decision-making. To evaluate this approach, we utilized a recently published dataset of a perceptual decision-making (Georgie et al., 2018).

2. Materials and methods

2.1. Experimental design

We employed a recently published decision-making dataset (Georgie et al., 2018), which included both the physiological (EEG and fMRI) and behavioral (RT and response correctness) data from seventeen members (8 females, 2 left-handed) of healthy adults aged 20–33 years at the University of Birmingham campus (Georgie et al., 2018). Participants categorized objects in a 2 × 2 factorial design task with the internal subject state (spatial prioritization) and external world state (stimulus coherency) factors (Fig. 1). At each trial, the scrambled image of a car or a face was presented on the right or left visual hemifield for 200 ms. Participants were asked to categorize objects as quickly and as accurately as possible by pressing their right or middle finger for selection in each category. For the first factor of the task design, the visual informativeness of the stimulus was manipulated by altering the phase of the images at the low and high coherency levels. For the spatial prioritization factor, a cueing arrow indicating the stimulus' visual hemifield was shown for 1000 ms before the stimulus presentation on half of the trials. In the other half of the trials, a two-sided cueing arrow was presented for 1000 ms. After the disappearance of the cueing arrow, the stimulus was presented randomly on each visual hemifield. These two factors created four different conditions: high coherency – prioritized (HCP), high coherency – not prioritized (HCNP), low coherency – prioritized (LCP), and low coherency – not prioritized (LCNP). For more information, refer to (Georgie et al., 2018).

2.2. Data acquisition

The data acquisition with the magnetic resonance (MR) scanner and simultaneous recording of EEG and fMRI included 90 trials for each condition with an intertrial interval of 10–12 s. These 90 trials were split into five separate experimental sessions. All EEG data were acquired with a 64-channel MR compatible EEG system. The scalp electrodes on the EEG cap followed the 10–20 system in naming and placement, including two additional channels, one for recording the electrocardiogram (ECG) and the other for recording the electrooculography (EOG).

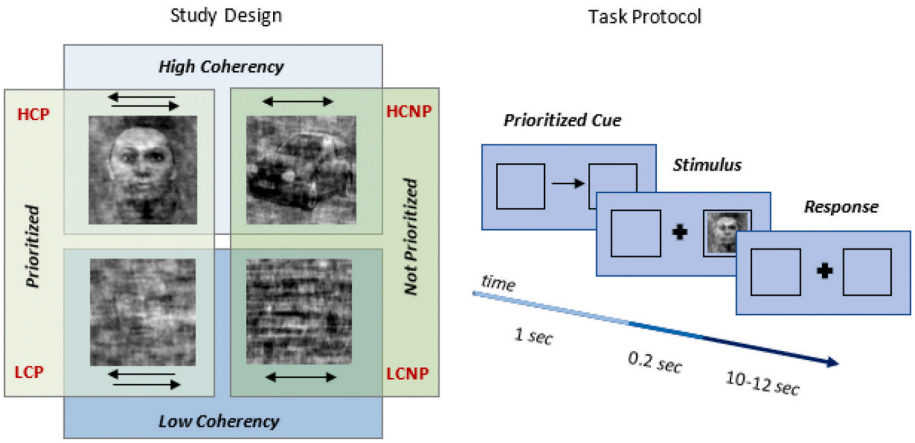

Fig. 1. Task protocol overview. A 2 × 2 factorial design task with spatial prioritization and stimulus coherency factors. At each trial, the scrambled image of a car or a face was presented on the right or left visual hemifield for 200 ms. For the coherency factor, the visual informativeness of the stimulus was manipulated by altering the phase of the images at low and high coherency levels. For the prioritization factor, a cueing arrow indicating the visual hemifield of the stimulus was shown for 1000 ms before the stimulus presentation on half of the trials.

2.3. Data preprocessing

We employed the re-referenced and MR-related artifact-free version of EEG data, which was provided by the owners. The EEG data were downsampled to 500Hz. Further data preprocessing was performed in this study using the Fieldtrip toolbox (Oostenveld et al., 2011). EEG data were bandpass filtered (a zero-phase, two-pass, and fourth-order Butterworth filter) from 1Hz to 70Hz, followed by band-stop filtering (a zero-phase, two-pass, and fourth-order Butterworth filter) from 48Hz to 52Hz. The significant artifactual EEG sections were selected visually and were ignored before further analysis. The eye movement and muscle artifacts were removed using independent component analysis (ICA). Accordingly, the artifactual components were selected visually and rejected from the components set, and the artifact-free data were obtained by reconstructing the refined ICA components. The stimulus-lock epochs with the length of RT were extracted from EEG data and were baseline corrected using the 200 ms pre-cue baseline (the time interval between 1200 ms and 1000 ms pre-stimulus). Of the initial total of 16 participants (one subject did not have behavioral data) with five sessions for each subject, five subjects were removed from further analysis because of the significantly poor EEG data quality. From the remaining sessions corresponding to the 11 subjects, a total of 13 sessions were rejected as well. Further analysis of both behavioral and physiological levels was applied to the remaining 43 sessions.

2.4. Behavioral data analysis

The drift-diffusion model (DDM) – a most discussed model for the evidence accumulation process – was employed to analyze the decision-making process at the behavioral level. The DDM views decision-making as a process of noisy accumulation of evidence over time (Fig. 2), which is commonly parameterized by a set of three parameters, i.e., drift rate, decision boundary, and bias. The average rate of accumulating the noisy evidence is called drift rate, *v*, which models the efficiency of the evidence accumulation. As such, more efficient evidence accumulation leads to higher drift rates (Beste et al., 2018). The higher drift rate is also associated with a faster decision-making process (Ratcliff and McKoon, 2008). In this model, the sensory evidence from perception accumulates over time until it reaches a decision boundary, *a,* for each choice. Models sometimes include a bias parameter, *z*, when there is some prior knowledge about the task. This model can separate the decision component from the non-decision ones, such as stimulus encoding and response execution (Ratcliff and McKoon, 2008; Ratcliff et al., 2016). These non-decision components together have a mean-time, t_{er}, which is called non-decision time. The decision component is also characterized by the drift rate parameter.

In this study, we evaluated the decision-making performance under

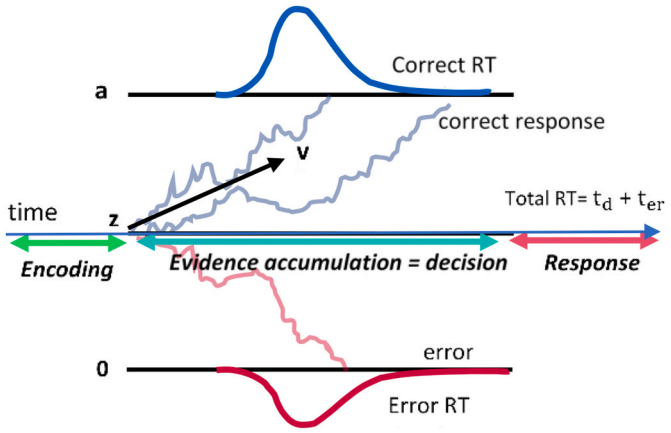

Fig. 2. The diffusion decision model. Noisy evidence is accumulated from the starting point, *z,* over time (during t_d *ms*) with the average drift rate, *v,* until it reaches the decision boundary, *a.* The non-decision components such as encoding and response output have a mean time called non-decision time, t_{er}. Thus, total RT includes non-decision time, t_{er}, and decision time, t_d.

different conditions. The hierarchical DDM (HDDM) (Wiecki et al., 2013) was employed to estimate model parameters *v*, *a* and t_{er}. Markov chain Monte Carlo (MCMC) sampling was employed to approximate the posterior probability of the model parameters at the individual and group levels. We initialized the HDDM with 10000 posterior samples and discarded the first 1000 samples as burn-in. The parameters of the HDDM were estimated separately for different conditions (HCP, HCNP, LCP, and LCNP) to show the effect of the coherency and spatial prioritization on decision-making performance. A two-way repeated measure analysis of variance (ANOVA) was then employed to test the effect of stimulus coherency and spatial prioritization on the decision and non-decision components of the DDM.

2.5. EEG data analysis

As mentioned before, the decision-making process consists of some processing stages, i.e., encoding, decision-making, and response execution. At the behavioral level, the encoding and response execution were considered a single non-decision component, characterized by the non-decision time parameter. The decision stage was also viewed as an evidence accumulation process described by the drift rate parameter. Uncovering the timing and the neural basis of these processing stages provides more insight into this process. In this study, we characterized the decision-making building blocks by employing the HSMM-EEG method (Borst and Anderson, 2015) at the physiological level. This

method is based on a hidden semi-Markov model that assigns each sample to one stage and determines the transition between the stages (Fig. 3). Using this method, we characterized each stage by duration and signature parameters. We used the windowed EEG signal naming snapshot instead of EEG samples to reduce the model complexity and represent the EEG data's temporal profile to the HSMM.

According to this method, each preprocessed trial was partitioned into equal-size snapshots. Each snapshot vector was created by concatenating the channel vectors of the EEG samples inside the window. These snapshots provided information about the average activity and the EEG data's temporal profile inside the window. A dimensionality reduction procedure was then performed by principal component analysis (PCA) of the combined snapshots (Fig. 3). We employed the first K components, which accommodated 98% of the variance of the data. Finally, the HSMM-EEG was fitted using the denoised low dimensional representation of the snapshots. For more details about the theoretical concept of the HSMM-EEG, please refer to (Borst and Anderson, 2015).

Using a snapshot length of 160 ms with 101 PCA components, which accounted for 98% of the total data variance, the data were analyzed to uncover three stages of the decision-making process. The two-way repeated measure ANOVA was then employed to test the association between coherency and prioritization factors and the duration of the stages. Relationships between behavioral and neural levels were also investigated using Pearson's correlation analysis.

3. Results

3.1. Decision-making characterization at the behavioral level

The coherency of the stimulus was changed at two different levels to influence the amount of sensory evidence. The spatial prioritization factor was also applied to change the attentional subject state. The participants were asked to categorize cars versus faces under the combination of these factors. The response time and response accuracy were analyzed to check the influence of these two factors on decision-making performance. The results of the two-way repeated measure ANOVA revealed the significant main effect of the coherency factor on the response time ($F_{(1,10)} = 92.12, p < 0.001$) and response accuracy ($F_{(1,10)} = 254.02, p < 0.001$). Thus, increasing the coherency level of the stimulus provided faster and more accurate responses (Fig. 4). The spatial prioritization also had a significant main effect on the response time ($F_{(1,10)} = 12.13, p = 0.006$), and the response accuracy ($F_{(1,10)} = 7.65, p = 0.02$). There were no significant interactions between coherency and spatial prioritization factors on reaction time ($F_{(1,10)} = 0.1, p = 0.76$) and response accuracy ($F_{(1,10)} = 3.1, p = 0.11$).

To further characterize the influence of the coherency and spatial prioritization on the decision-making process, the decision and non-decision components of this process were estimated using DDM. We hypothesized that the decision component of the process was the only processing stage associated with stimulus coherency and spatial prioritization factors. We also showed that the coherency factor had a stronger

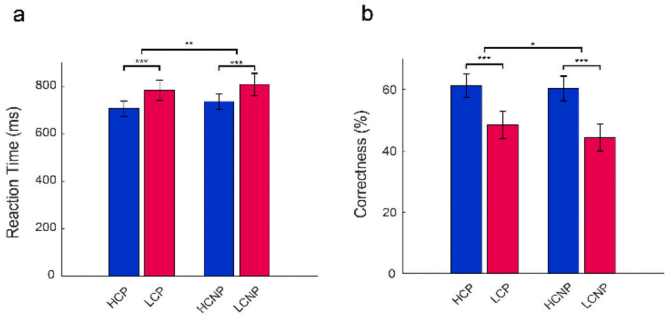

Fig. 4. Mean response time and response accuracy across subjects. a. demonstrates the mean response time across subjects for each condition. The two-way repeated measure ANOVA revealed the significant main effect of the coherency ($F_{(1,10)} = 92.12, p < 0.001$) and spatial prioritization ($F_{(1,10)} = 12.13, p = 0.006$) factors on the response time. b. illustrates the mean response correctness across subjects for each condition. The results show a significant main effect of coherency ($F_{(1,10)} = 254.02, p < 0.001$) and spatial prioritization ($F_{(1,10)} = 7.65, p = 0.02$) on the response accuracy. The signs '***', '**' and '*' symbolize p-value < 0.001, p-value < 0.01, and p-value < 0.05 respectively.

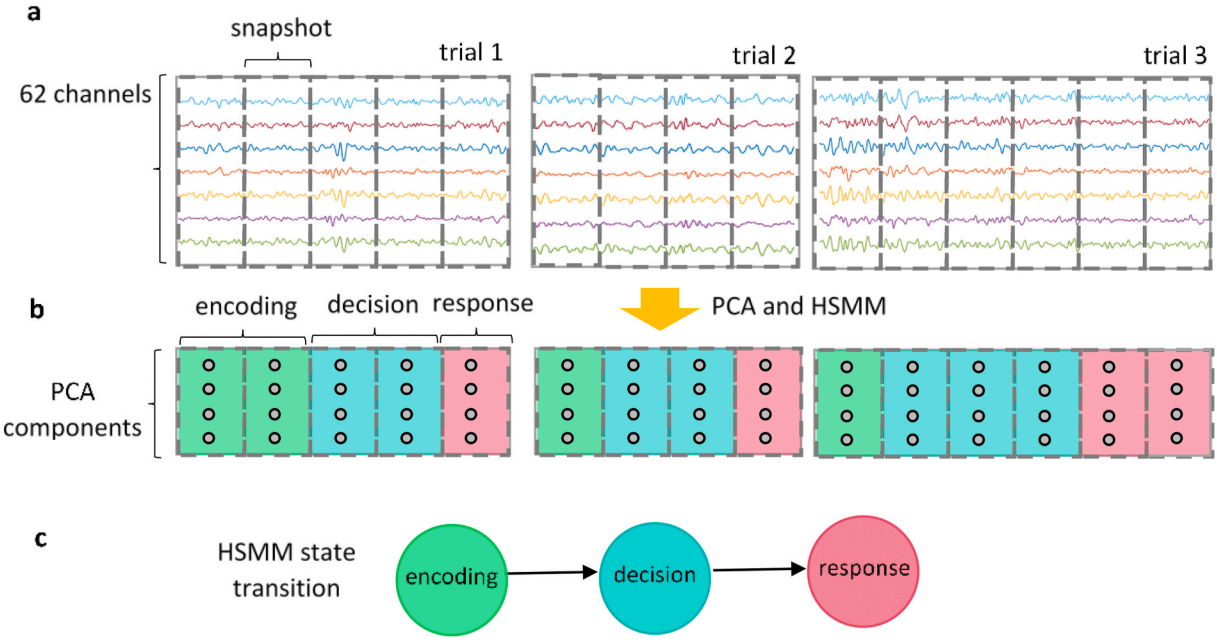

Fig. 3. Information processing stages extraction using HSMM-EEG analysis. a. Shows windowing EEG signals to create snapshots. **b.** The snapshots are pre-processed to reduce dimensionality. The preprocessed snapshots are fed to the HSMM-EEG to separate decision-making stages. The results of the HSMM-EEG on the snapshots are shown with three colors for encoding (green), decision (blue), and response (red). **c.** Illustration of the HSMM-EEG stage transition with encoding, decision, and response stages. (For interpretation of the references to color in this figure legend, the reader is referred to the Web version of this article.)

relationship with evidence accumulation than the prioritization factor.

To test this hypothesis at the behavioral level, the drift rate and non-decision time parameters of the DDM were estimated for each condition (HCP, HCNP, LCP, and LCNP). These two parameters characterized the decision and non-decision components of the process, respectively. The results of the statistical test demonstrated that coherency and spatial prioritization significantly affected the drift rate parameter, as determined by two-way repeated measure ANOVA ($F_{(1,10)}$= 496.79, $p <$ 0.001) (Fig. 5). Moreover, we found a significant effect of the prioritization factor on the drift rate ($F_{(1,10)} = 6.9$, $p = 0.03$). As expected, the results revealed the major impact of the coherency and spatial prioritization factors on the efficiency of evidence accumulation rather than the spatial prioritization factor. The analysis showed no significant interaction ($F_{(1,10)} = 0.03$, $p = 0.88$) between coherency and spatial prioritization on the drift rate. Additionally, we checked whether the coherency and spatial prioritization were associated with the non-decision component. As depicted in Fig. 5, the two-way repeated measure ANOVA disclosed no significant main effect of the stimulus coherency ($F_{(1,10)}$= 0.39, $p = 0.55$) and spatial prioritization ($F_{(1,10)} = 0.05$, $p = 0.83$) factors on the non-decision time parameter. There was also no significant interaction ($F_{(1,10)} = 0.9$, $p = 0.37$) between these two factors on the non-decision time.

Overall, the results demonstrated that only evidence accumulation is related to stimulus coherency and spatial prioritization among the different processing stages of decision-making. Since the non-decision component was not associated with factors of interest, the efficiency of the decision-making process was more dependent on the evidence accumulation stage.

3.2. Decision-making characterization at the neural level

Next, we investigated whether we could characterize the decision-making process in more detail by estimating the timing and neural signature of the individual processing stage. With the benefit of EEG data with millisecond temporal resolution and the use of the HSMM-EEG method, we extracted the timing of each processing stage for each condition, i.e., HCP, HCNP, LCP, and LCNP (Fig. 6). Since the sequences of the stages were the same for all conditions, the conditions were analyzed jointly with HSMM-EEG. Using the duration of the processing stages, we tested the previous hypothesis and checked whether coherency and spatial prioritization were associated with the duration of the cognitive stages. As shown in Fig. 6, the two-way repeated measure ANOVA found no significant main effect of stimulus coherency ($F_{(1,10)} =$ 0.37, $p = 0.56$) and spatial prioritization ($F_{(1,10)} = 0.55$, $p = 0.48$) factors on the encoding stage duration. The results also revealed no significant interaction ($F_{(1,10)} = 2.03$, $p = 0.18$) between coherency and spatial prioritization on the encoding state duration. As expected, the coherency had a significant main effect on the duration of the decision stage as determined by two-way repeated measure ANOVA ($F_{(1,10)} =$ 31.85, $p = 0.002$). However, this analysis disclosed no significant effect of spatial prioritization ($F_{(1,10)} = 3.25$, $p = 0.1$) on the duration of the decision stage. Additionally, the coherency and spatial prioritization did not have any significant interaction on this stage ($F_{(1,10)} = 0.14$, $p =$ 0.72). The response execution stage was also analyzed by the two-way repeated measure ANOVA to find the impacts of coherency and prioritization factors on the duration of this stage. The results of the statistical test revealed that there was a significant main effect of coherency ($F_{(1,10)}$ = 6.22, $p = 0.03$) on response duration. However, this analysis found that the spatial prioritization did not have a significant impact ($F_{(1,10)} =$ 0.01, $p = 0.94$) on this stage. Furthermore, there was no significant interaction ($F_{(1,10)} = 1.44$, $p = 0.26$) between these two factors on the response duration. As expected, the overall results demonstrated that decision-making was more affected by the coherency factor than spatial prioritization. This strong association was more visible in the decision stage duration because reducing the coherency level increased the required time to accumulate evidence to reach the decision boundary.

To further characterize the decision-making process, the signatures of the processing stages were computed by taking the weighted average of the snapshots across trials. Each snapshot's weight was the probability of belonging to that snapshot to each state estimated by the HSMM-EEG. The resulting signatures are illustrated in Fig. 7. As shown in this figure, the occipital negativity was observed at the encoding stage. It was consistent with previous findings that the posterior visual N200 component of the event-related potential (ERP) was associated with the sensory processing (Patel and Azzam, 2005; Portellaet al., 2012; Nunez et al., 2019). At the next two stages, the encoded evidence accumulated over time to reach the decision boundary and finalize the response execution. The signature of the decision and response stages revealed the CPP's increase at the decision and response execution stages. Previous research also disclosed the increase of the CPP with incoming evidence that peaked at response execution time (O'Connell et al., 1729; Tagliabue et al., 2019). The neural basis of response execution clarified the positivity of the left motor cortex as well. It might be because as most of the subjects were right-handed (9 of 11 subjects), the left motor cortex' activity was increased at the response execution stage.

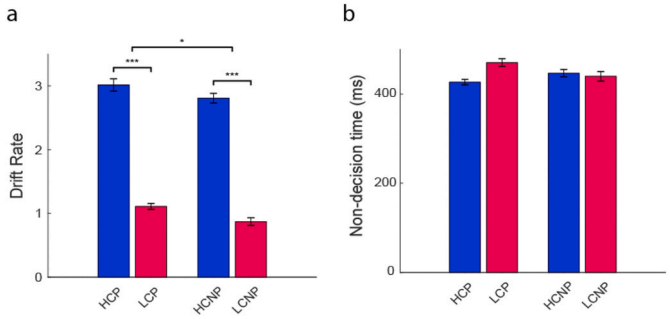

Fig. 5. The predicted drift rate and non-decision time. a. Illustration of the mean of the drift rate parameter across subjects for different conditions (HCP, HCNP, LCP, and LCNP). The significant main effect of the coherency factor was reported by two-way repeated measure ANOVA ($F_{(1,10)}$ = 496.79, $p <$ 0.001). Moreover, a significant difference was found by the prioritization factor by two-way repeated measure ANOVA ($F_{(1,10)}$ = 6.9, p = 0.03). **b.** Presentation of the mean of the non-decision time parameter across subjects for each condition. There was no significant main effect of coherency ($F_{(1,10)}$ = 0.39, p = 0.55) and prioritization factors ($F_{(1,10)}$ = 0.05, p = 0.83) on this parameter as reported by two-way repeated measure ANOVA. Error bars represent the standard error of the mean. The signs '***' and '*' symbolize p-value < 0.001 and p-value < 0.05 respectively.

3.3. Brain-behavior relationships

We investigated the association between behavioral and neural representations of the decision-making process. At the behavioral level, the DDM considers the drift rate and non-decision time parameters to describe the decision and non-decision stages of the process. Additionally, the HSSM-EEG method decomposes the decision-making process into its components at the physiological level by estimating each processing stage's timing. We examined the association between DDM parameters and the duration of the information processing stages to probe the relationships between decision-making characterization at the physiological and behavioral levels.

As reported with previous research, faster decisions were associated with a higher drift rate (Ratcliff and McKoon, 2008). Thus, we investigated whether the drift rate parameter had a negative interaction with the duration of the decision stage at the physiological level. Fig. 9a indicates the estimated drift rate and duration of the decision stage for each condition. A significant negative correlation ($r = -0.47$, $p = 0.001$, Pearson's correlation) was found between the decision stage's

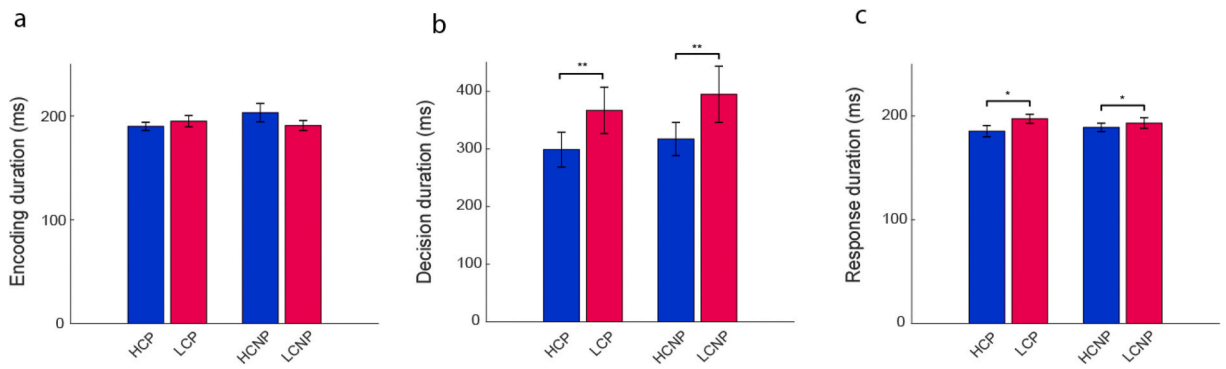

Fig. 6. Estimated processing stages duration. Illustration of the mean timing of decision-making stages, i.e., encoding, decision, and response for individual conditions (HCP, HCNP, LCNP, and LCNP). The two-way repeated measure ANOVA found no significant main effect of coherency ($F_{(1,10)} = 0.37$, $p = 0.56$) and spatial prioritization ($F_{(1,10)} = 0.55$, $p = 0.48$) on the duration of the encoding stage. The significant effect of the coherency was found by the two-way repeated measure ANOVA on the decision stage duration ($F_{(1,10)} = 31.85$, $p = 0.002$). However, there was no significant association between the decision stage and the prioritization factor ($F_{(1,10)} = 3.25$, $p = 0.1$), as determined by ANOVA. Finally, the statistical analysis found a significant effect of coherency ($F_{(1,10)} = 6.22$, $p = 0.03$) on the response duration. While, the prioritization did not have a significant main effect ($F_{(1,10)} = 0.01$, $p = 0.94$) on this state. Error bars represent standard error of the mean. The signs '**' and '*' symbolize p-value < 0.01 and p-value < 0.05.

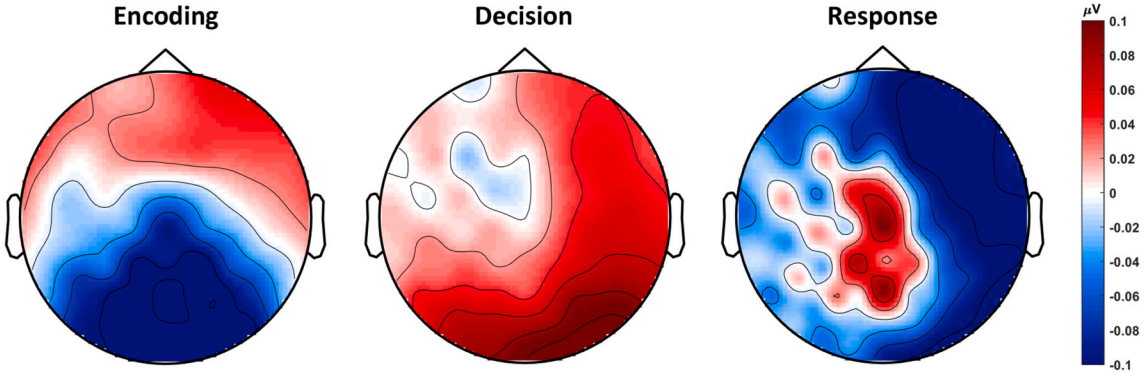

Fig. 7. Signature of the processing stages. The signatures were created by taking the weighted average of the snapshots across trials. **a.** The signature of the encoding stage disclosed the negativity of the visual areas. **b** and **c** illustrate the decision and response stages, respectively. The signature of these two stages demonstrated the increase of CPP until response execution. The positivity of the left motor cortex was also depicted at the response execution stage.

physiological and behavioral characterizations, which was consistent with the previous findings (Ratcliff and McKoon, 2008). Additionally, we checked whether the non-decision parts of the decision process had any interaction between brain and behavior representations. Fig. 9b shows the non-decision time parameter estimated by the DDM. The sum of the duration of encoding and response stages resulted from the HSSM-EEG model for each condition. The results demonstrated a significant positive interaction ($r = 0.78$, $p < 0.001$, Pearson's correlation) between behavioral and physiological representations of the non-decision component.

We further examined the relationships between physiological representation of the decision-making process and the RT. We hypothesized that the entire decision-making process' duration depended more on the decision stage rather than the non-decision stages. To test this hypothesis, the interaction between each stage duration with the RT was estimated using Pearson's correlation across subjects and conditions (Fig. 9). A significant interaction was found between the duration of the decision stage and RT ($r = 0.99$, $p < 0.001$, Pearson's correlation). The correlation analysis revealed no significant interactions between RT and duration of the encoding ($r = 0.25$, $p = 0.11$, Pearson's correlation) and response ($r = 0.29$, $p = 0.06$, Pearson's correlation) stages. The results disclosed that the most important factor in RT is the duration of the evidence accumulation process. Such that the faster accumulation process led to shorter reaction times.

4. Discussion

The classical model of the decision-making process encompasses three distinct processing stages, i.e., encoding, decision, and response execution. Our analysis shed light on the decision-making process by characterizing/linking this process at both neural and behavioral levels. At the neural level with the aim of EEG data with a high temporal resolution, the timing and neural signature of the processing stages of the decision-making process (encoding, decision, and response execution) were estimated. Taken together, the relationship between the behavioral data and different stages of the decision-making process on EEG provides insights into the underlying process. Using the HSMM-EEG model, the decision-making process stages were extracted associated with the duration and neural signature parameters (Figs. 6 and 7). The encoding stage's duration, depicted in Fig. 6a, revealed that the time needed for sensory inputs to be encoded was nearly 190 ms. This is consistent with the previous study, which clarified that the latency of the N200 component of the ERP reflected the time of sensory encoding (Nunez et al., 2019). The previous animal studies also revealed that the LIP neurons started to accumulate the perceptual evidence about 200 ms after stimulus presentation (Roitman and Shadlen, 2002). During the encoding stage, the occipital negativity was observed in the visual area (Fig. 7a). As reported by recent studies (Patel and Azzam, 2005; Portellaet al., 2012; Nunez et al., 2019), the N200 component at the visual area was associated with perceptual processing, which is in line

with our result. The MEG study on the frequency domain also disclosed the gamma band activity on the visual cortex as the stimulus encoding (Siegel et al., 2011). At the decision stage, the encoded sensory inputs were accumulated to reach the decision boundary. The decision stage's neural signature revealed the increase of the CPP in the decision and response stages (Fig. 7b and c).

Similarly, previous studies found that CPP was associated with the evidence accumulation process with a pick at the response execution time (O'Connell et al., 1729; van Vugt et al., 1715; Kelly and O'Connell, 2013; Tagliabue et al., 2019), which confirms the resultant signatures. When the accumulated perceptual evidence reached the decision boundary, the motor execution was initiated. As shown in the signature of the response stage (Fig. 7c), besides increasing the CPP, the left motor cortex' positivity was observed as well. It was because most of the participants were right-handed (9 of 11 subjects). The processing at the motor execution stage, on average, lasted about 190 ms, as depicted in Fig. 6c. The MEG study revealed that event-related desynchronization (ERD) peaked about 170 ms before response execution over the sensorimotor area contralateral to the response side (Kaiser et al., 2006).

Further analyses were applied to check whether the coherency and spatial prioritization were associated with the decision-making components at both behavioral and physiological levels. Statistical analysis at the behavioral level revealed that the reaction time and response accuracy were more associated with the coherency factor. Such that conditions with higher stimulus coherency had more accurate and faster reaction times. These findings align with the studies' results on the decision-making process (Roitman and Shadlen, 2002; Gold and Shadlen, 2000/03; Liu and Pleskac, 2011; Pedersen et al., 2015). The spatial prioritization factor also had an impact on the performance of the decision-making process. Accordingly, trials with spatial prioritization had faster reaction times and more accurate responses. In line with our results, recent studies demonstrated that attentional cues led to higher accuracy and faster responses (van Ede et al., 2012; Mulder and van Maaneneng, 2013). Other analyses in our research that were performed with DDM at the behavioral level also revealed the impact of these factors on the decision-making process. Our findings indicated that the drift rate was associated with the coherency factor. The effect of the stimulus coherency on the drift rate confirmed this parameter's role as a perceptual input quality measure, as explained by the DDM (Ratcliff, 2014). The analysis of the single set recordings also supported this finding; it showed that faster responses were associated with the rapid build-up of activity of the LIP (Roitman and Shadlen, 2002), FEF (Mante et al., 2013/11), striatum (Ding and Gold, 2010), and superior colliculus (Horwitz and Newsome, 1999) neurons.

Similar analyses were applied to the duration of the cognitive stages at the physiological level. As expected from the behavioral analysis findings, the coherency was more associated with the decision stage course than others. The investigation of the decision-making process at the physiological level also confirmed the findings of behavioral analysis. The results demonstrated that decision-making is affected by the coherency factor rather than spatial prioritization. Changing the coherency level of the stimulus had only an association with the decision stage duration. It might be because stimulus coherency affected the input sensory evidence quality. Therefore, lower stimulus coherency needed more time to reach the decision boundary characterized by the evidence accumulation process. The findings from both behavioral and physiological levels also disclosed that the decision-making process was more dependent on the decision stage than non-decision ones. To support this hypothesis, we also analyzed the relationships between the duration of processing stages and RT, as depicted in Fig. 9. As expected, the results revealed that RT was more associated with the decision stage's duration than others. This relationship also demonstrated the importance of this stage at the speed of the decision-making process.

According to the similar operation of the decision-making process' neural and behavioral representations under task conditions, we tested whether there was a relationship between these two levels (Fig. 8). Consequently, we hypothesized that the drift rate parameter that characterized the efficiency of the evidence accumulation process had an interaction with the decision stage's duration at the physiological level. As such, higher drift rates provided shorter decision stages. Similarly, we tested whether the duration of the combination of the encoding and response stages had any interaction with the non-decision time of the DDM. To test these hypotheses, Pearson's correlation was conducted, and the results confirmed the significant association between physiological and behavioral levels. Our findings were consistent with the studies on the evidence accumulation process, as mentioned earlier (Ratcliff and McKoon, 2008; Roitman and Shadlen, 2002; Mante et al., 2013/11; Horwitz and Newsome, 1999). According to these studies, more coherent evidence was accumulated faster to reach the decision boundary. So, higher drift rates were associated with the shorter decision duration.

5. Conclusion

In this study, we sought to bridge the gap between neural and behavioral representations of the decision-making process. Neural characterization of the decision-making process was uncovered through information processing stages. We showed that these two

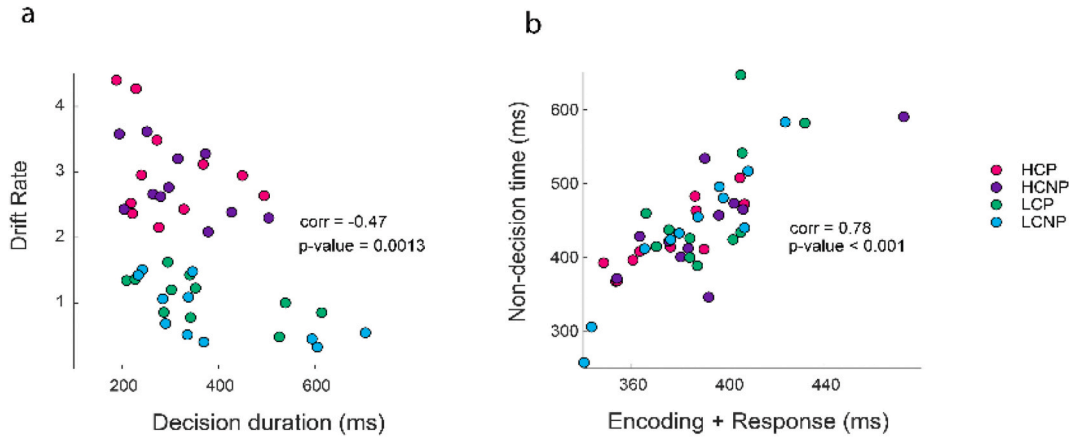

Fig. 8. Association between behavioral and physiological representations of the decision-making process. a. Shows the interaction between the drift rate parameter of the DDM and the decision stage duration of the HSMM-EEG model for each condition. The significant negative interaction ($r = -0.47$, $p = 0.001$, Pearson's correlation) was found between these parameters. **b.** Illustrates the non-decision time and sum of encoding and response stages duration for each condition. The results clarified a significant positive correlation ($r = 0.78$, $p < 0.001$, Pearson's correlation) between these parameters.

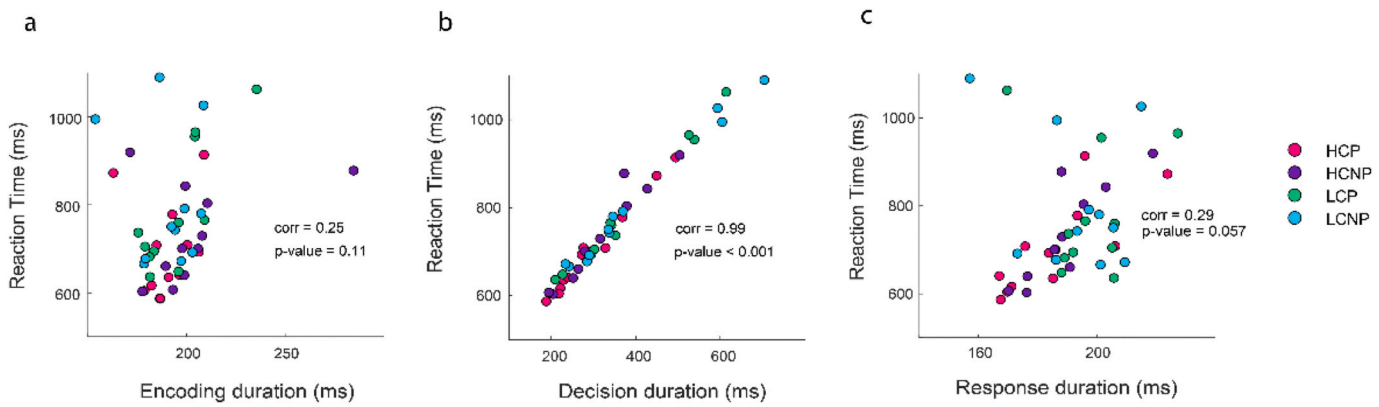

Fig. 9. Relationships between reaction time and decision stages duration. Panels a, b, and c depict the mean value of the RT and the encoding, decision, and response duration respectively for each subject and condition. A significant interaction was found between the RT and duration of encoding ($r = 0.25$, $p = 0.11$, Pearson's correlation), decision ($r = 0.99$, $p < 0.001$, Pearson's correlation), and response ($r = 0.29$, $p = 0.06$, Pearson's correlation) states.

representations had a similar manner under different stimulus coherency levels. Additionally, the results at both neural and behavioral levels revealed the importance of the decision stage on the efficiency of the whole decision-making process. The significant association between processing components at both neural and behavioral levels was also a validation for the neural characterization of the decision-making process. Overall, our results demonstrated that this representation provided more insight into the decision-making process by providing both the cognitive stages' duration and neural signature. We showed that at each processing stage, several brain areas activated for encoding, accumulating the evidence, and response execution. Using the brain area activity at each processing stage, one can extract the information flow between areas at each stage. It is also possible to decompose the whole cognitive process to multiple states with a specific synchronization pattern (Vidaurreet al., 2018/07). Since decision-making is a distributed process with interactions among multiple brain areas despite the canonical model of decision-making, incorporating the area synchronization and communication at the modeling of the decision-making process will provide a better understanding of this process.

Credit roles

M.M.G. and E.I. performed conceptualization, methodology development, writing, and revision of the paper; E.I. analyzed data; A.H. contributed to methodology development and editing; H.P. contributed to editing and reviewing; M.M.G., A.H., and H.P. supervised the project.

Acknowledgments

All data used in this research is publicly available in the open science framework (https://osf.io/). We would like to thank Dr. Dirk Ostwald and his colleagues that make this data publicly available. This research is supported by Cognitive Science and Technology Council of Iran.

References

Anderson, J.R., Zhang, Q., Borst, J.P., Walsh, M.M., 2016. The discovery of processing stages: extension of Sternberg's method. Psychol. Rev. 123 (5), 481–509.
Beste, C., Adelhöfer, N., Gohil, K., Passow, S., Roessner, V., Li, S.-C., 2018. Dopamine modulates the efficiency of sensory evidence accumulation during perceptual decision making. in eng), The international journal of neuropsychopharmacology 21 (7), 649–655.
Binder, J.R., Liebenthal, E., Possing, E.T., Medler, D.A., Ward, B.D., 2004/03/01 2004. Neural correlates of sensory and decision processes in auditory object identification. Nat. Neurosci. 7 (3), 295–301.
Borst, J.P., Anderson, J.R., 2015. The discovery of processing stages: analyzing EEG data with hidden semi-Markov models. Neuroimage 108, 60–73.
Brown, S.D., Heathcote, A., 2008/11/01/2008. The simplest complete model of choice response time: linear ballistic accumulation. Cognit. Psychol. 57 (3), 153–178.
J. F. Cavanagh et al., "Subthalamic nucleus stimulation reverses mediofrontal influence over decision threshold," Nat. Neurosci., vol. 14, no. 11, pp. 1462-1467, 2011/11/01 2011.
Ding, L., Gold, J.I., 2010. Caudate Encodes Multiple Computations for Perceptual Decisions 30 (47), 15747–15759.
T. H. Donner, M. Siegel, P. Fries, and A. K. Engel, "Buildup of choice-predictive activity in human motor cortex during perceptual decision making," Curr. Biol., vol. 19, no. 18, pp. 1581-1585, 2009/09/29/2009.
Forstmann, B.U., et al., 2008. Striatum and pre-SMA facilitate decision-making under time pressure, 105 (45), 17538–17542.
Georgie, Y.K., Porcaro, C., Mayhew, S., Bagshaw, A.P., Ostwald, D., 2018. A Perceptual Decision Making EEG/fMRI Data Set, p. 253047 bioRxiv.
Gold, J.I., Shadlen, M.N., 2000/03/01 2000. Representation of a perceptual decision in developing oculomotor commands. Nature 404 (6776), 390–394.
Gold, J.I., Shadlen, M.N., 2001. Neural computations that underlie decisions about sensory stimuli. Trends Cognit. Sci. 5 (1), 10–16.
Grinband, J., Hirsch, J., Ferrera, V.P., 2006/03/02/2006. A neural representation of categorization uncertainty in the human brain. Neuron 49 (5), 757–763.
Hanks, T.D., Summerfield, C., 2017/01/04/2017. Perceptual decision making in rodents, monkeys, and humans. Neuron 93 (1), 15–31.
Hanks, T.D., Kopec, C.D., Brunton, B.W., Duan, C.A., Erlich, J.C., Brody, C.D.J.N., 2015. Distinct relationships of parietal and prefrontal cortices to evidence accumulation, 520 (7546), 220–223.
Heekeren, H.R., Marrett, S., Bandettini, P.A., Ungerleider, L.G., 2004/10/01 2004. A general mechanism for perceptual decision-making in the human brain. Nature 431, 859–862, 7010.
Herz, Damian M., Zavala, Baltazar A., Bogacz, R., Brown, P., 2016. Neural correlates of decision thresholds in the human subthalamic nucleus. Curr. Biol. 26 (7), 916–920.
Ho, T.C., Brown, S., Serences, J.T., 2009. Domain general mechanisms of perceptual decision making in human cortex, 29 (27), 8675–8687.
Horwitz, G.D., Newsome, W.T., 1999. Separate signals for target selection and movement specification in the superior colliculus, 284 (5417), 1158–1161.
Kaiser, J., Lennert, T., Lutzenberger, W., 2006. Dynamics of oscillatory activity during auditory decision making. Cerebr. Cortex 17 (10), 2258–2267.
Kelly, S.P., O'Connell, R.G., 2013. Internal and external influences on the rate of sensory evidence accumulation in the human brain, 33 (50), 19434–19441.
Liu, T., Pleskac, T.J., 2011. Neural correlates of evidence accumulation in a perceptual decision task, 106 (5), 2383–2398.
Mante, V., Sussillo, D., Shenoy, K.V., Newsome, W.T., 2013/11/01 2013. Context-dependent computation by recurrent dynamics in prefrontal cortex. Nature 503 (7474), 78–84.
Mulder, M.J., van Maanen, L., 2013. Are accuracy and reaction time affected via different processes? In: eng (Ed.), PloS One 8 (11), e80222 e80222.
Mulder, M., Van Maanen, L., Forstmann, B., 2014. Perceptual decision neurosciences–a model-based review. Neuroscience 277, 872–884.
M. D. Nunez, A. Gosai, J. Vandekerckhove, and R. Srinivasan, "The latency of a visual evoked potential tracks the onset of decision making," Neuroimage, vol. 197, pp. 93-108, 2019/08/15/2019.
R. G. O'Connell, P. M. Dockree, and S. P. Kelly, "A supramodal accumulation-to-bound signal that determines perceptual decisions in humans," Nat. Neurosci., vol. 15, no. 12, pp. 1729-1735, 2012/12/01 2012.
Oostenveld, R., Fries, P., Maris, E., Schoffelen, J.-M.J. C. i., 2011. neuroscience, "FieldTrip: open source software for advanced analysis of MEG, EEG, and invasive electrophysiological data. Comput. Intell. Neurosci. 1, 2011.
Patel, S.H., Azzam, P.N., 2005. Characterization of N200 and P300: selected studies of the event-related potential. in eng), International journal of medical sciences 2 (4), 147–154.
Pedersen, M.L., Endestad, T., Biele, G.J. P.o., 2015. Evidence accumulation and choice maintenance are dissociated in human perceptual decision making, 10 (10).
Philiastides, M.G., Sajda, P., 2007. EEG-informed fMRI reveals spatiotemporal characteristics of perceptual decision making, 27 (48), 13082–13091.

Pisauro, M.A., Fouragnan, E., Retzler, C., Philiastides, M.G., 2017. Neural correlates of evidence accumulation during value-based decisions revealed via simultaneous EEG-fMRI. Nat. Commun. 8, 15808.
Portella, C., et al., 2012. Relationship between early and late stages of information processing: an event-related potential study. Neurol. Int. 4 (3).
Ratcliff, R., 2014. Measuring psychometric functions with the diffusion model. in eng), Journal of experimental psychology. Human perception and performance 40 (2), 870–888.
Ratcliff, R., McKoon, G., 2008. The diffusion decision model: theory and data for two-choice decision tasks. Neural Comput. 20 (4), 873–922.
Ratcliff, R., Smith, P.L., 2004. A comparison of sequential sampling models for two-choice reaction time. Psychol. Rev. 111 (2), 333–367.
R. Ratcliff, P. L. Smith, S. D. Brown, and G. McKoon, "Diffusion decision model: current issues and history," Trends Cognit. Sci., vol. 20, no. 4, pp. 260-281, 2016/04/01/ 2016.
Roitman, J.D., Shadlen, M.N., 2002. Response of neurons in the lateral intraparietal area during a combined visual discrimination reaction time task. in eng), The Journal of neuroscience : the official journal of the Society for Neuroscience 22 (21), 9475–9489.
Scott, B.B., Constantinople, C.M., Akrami, A., Hanks, T.D., Brody, C.D., Tank, D.W.J.N., 2017. Fronto-parietal cortical circuits encode accumulated evidence with a diversity of timescales, 95 (2), 385–398 e5.
Siegel, M., Engel, A., Donner, T., 2011. Cortical network dynamics of perceptual decision-making in the human brain (in English). Review 5 (21). February-28 2011.
Smith, P.L., Ratcliff, R., 2004. Psychology and neurobiology of simple decisions. Trends Neurosci. 27 (3), 161–168.
Steinmetz, N.A., Zatka-Haas, P., Carandini, M., Harris, K.D., 2019/12/01 2019. Distributed coding of choice, action and engagement across the mouse brain. Nature 576 (7786), 266–273.
Sterzer, P., 2016. Moving forward in perceptual decision making, 113 (21), 5771–5773.
Stevner, A.B.A., et al., 2019/03/04 2019. Discovery of key whole-brain transitions and dynamics during human wakefulness and non-REM sleep. Nat. Commun. 10 (1), 1035.
C. F. Tagliabue, D. Veniero, C. S. Y. Benwell, R. Cecere, S. Savazzi, and G. Thut, "The EEG signature of sensory evidence accumulation during decision formation closely tracks subjective perceptual experience," Sci. Rep., vol. 9, no. 1, p. 4949, 2019/03/20 2019.
Usher, M., McClelland, J.L., 2001. The time course of perceptual choice: the leaky, competing accumulator model. Psychol. Rev. 108 (3), 550–592.
van Ede, F., de Lange, F.P., Maris, E., 2012. Attentional cues affect accuracy and reaction time via different cognitive and neural processes. in eng), The Journal of neuroscience : the official journal of the Society for Neuroscience 32 (30), 10408–10412.
van Maanen, L., et al., 2011. Neural correlates of trial-to-trial fluctuations in response caution. J. Neurosci. 31 (48), 17488–17495.
M. K. van Vugt, M. A. Beulen, and N. A. Taatgen, "Relation between centro-parietal positivity and diffusion model parameters in both perceptual and memory-based decision making," Brain Res., vol. 1715, pp. 1-12, 2019/07/15/2019.
M. van Vugt, P. Simen, L. Nystrom, P. Holmes, and J. Cohen, "EEG oscillations reveal neural correlates of evidence accumulation," (in English), Original Research vol. 6, no. 106, 2012-July-17 2012.
Veen, V.v., Krug, M.K., Carter, C.S., 2008. The neural and computational basis of controlled speed-accuracy tradeoff during task performance, 20 (11), 1952–1965.
Vidaurre, D., Quinn, A.J., Baker, A.P., Dupret, D., Tejero-Cantero, A., Woolrich, M.W., 2016. Spectrally resolved fast transient brain states in electrophysiological data. Neuroimage 126, 81–95.
Vidaurre, D., Myers, N.E., Stokes, M., Nobre, A.C., Woolrich, M.W.J.C.C., 2019. Temporally unconstrained decoding reveals consistent but time-varying stages of stimulus processing, 29 (2), 863–874.
Vidaurre, D., et al., 2018/07/30 2018. Spontaneous cortical activity transiently organises into frequency specific phase-coupling networks. Nat. Commun. 9 (1), 2987.
White, C.N., et al., 2014. Decomposing decision components in the stop-signal task: a model-based approach to individual differences in inhibitory control. in eng), Journal of cognitive neuroscience 26 (8), 1601–1614.
T. Wiecki, I. Sofer, and M. Frank, "HDDM: hierarchical bayesian estimation of the drift-diffusion model in Python," (in English), Methods vol. 7, no. 14, 2013-August-02 2013.
Winkel, J., et al., 2012-August-30 2012. Bromocriptine does not alter speed–accuracy tradeoff. Original Research 6 (126) (in English).
Zatka-Haas, P., Steinmetz, N.A., Carandini, M., Harris, K.D., 2018. Distinct Contributions of Mouse Cortical Areas to Visual Discrimination, p. 501627.